metals

MDPI

Article

Investigation of Structure and Mechanical Characteristics of a High Manganese Steel via SolidCast Simulation Method

Hussein Alrobei [1,*], Rizwan Ahmed Malik [2], Farhan Amjad [2] and Ibrahim AlBaijan [1]

[1] Department of Mechanical Engineering, College of Engineering, Prince Sattam bin Abdulaziz University, Al-Karj 11942, Saudi Arabia
[2] Department of Metallurgy and Materials Engineering, Faculty of Mechanical and Aeronautical Engineering, University of Engineering and Technology, Taxila 47050, Pakistan
* Correspondence: h.alrobei@psau.edu.sa

Abstract: Casting is a fabrication method used to create various industrial parts with different shapes. Flaws such as shrinkage, porosity, and short metal filling can result in casting rejection. These flaws are heavily reliant on casting parameter design (gating and riser system design) and can be reduced by optimizing the casting parameter design. The development of materials with new or improved properties has long been the primary objective of materials scientists. The designing of metallic alloys for structural purposes must take strength, toughness, and formability into account to achieve the desired performance. The unique convergence of these essential characteristics that characterize high manganese steels fascinate scientists worldwide. The current work systematically investigated a gating system and riser design effect for high Manganese steel samples (bushes) to develop an understanding of the structure–property relationship. The first conventional manual calculation was performed to design the gating and riser system. Subsequently, a sophisticated simulation software called SolidCast was used to design, validate, and improve the casting parameters of the specimen. To back up the findings, confirmatory experiments were carried out. Both designs were used to make castings in order to check for flaws. The microstructural and mechanical characteristics of these materials were investigated. Visual inspection of the manually-designed castings revealed considerable shrinkage, whereas software-designed castings seemed in good shape, without the shrinkage, macroporosity, and microporosity. The microstructure of the specimens was also studied by applying optical microscopy and SEM analysis. By improving the gating and riser system with the SolidCast software, sound casting was achieved. This improved the quality of casting results with a considerable enhancement of yield strength (~32 percent), hardness (~34 percent), and tensile strength (~27 percent), which may lead to significant cost savings.

Keywords: tensile testing; SolidCast simulation; structural analysis; high manganese steel

check for updates

Citation: Alrobei, H.; Malik, R.A.; Amjad, F.; AlBaijan, I. Investigation of Structure and Mechanical Characteristics of a High Manganese Steel via SolidCast Simulation Method. *Metals* **2023**, *13*, 572. https://doi.org/10.3390/met13030572

Academic Editors: Gunter Gerbeth and Wenchao Yang

Received: 13 December 2022
Revised: 4 March 2023
Accepted: 6 March 2023
Published: 12 March 2023

Copyright: © 2023 by the authors. Licensee MDPI, Basel, Switzerland. This article is an open access article distributed under the terms and conditions of the Creative Commons Attribution (CC BY) license (https://creativecommons.org/licenses/by/4.0/).

1. Introduction

For many years, the main goal of materials scientists has been the creation of materials with novel or enhanced characteristics. Steel is arguably the most significant structural material, currently. To generate and/or customize novel steels that are suitable for the widest range of applications, several design concepts have been created. Strength, toughness, and formability are crucial factors to consider to obtain the desired performance when designing metallic alloys for structural applications. Researchers worldwide are fascinated by high manganese steels owing to their unique combination of these properties.

Hadfield steel, or high manganese steel, first emerged decades earlier and was invented in 1882 by Sir Robert Hadfield. Industrial uses for this particular steel included impact hammers, jaws for crushers, liners for grinding mills, tractor crawler treads, and railroad crossings [1]. High manganese steel was primarily comprised of manganese (Mn) and carbon (C). Although manganese steel occasionally included almost 18% of Mn [2], which

stabilized the austenite phase and enriched the solid solution, conventional concentrations were ~0.7–1.45% of C and ~11–14% of Mn. Additionally, Mn increased the toughness of steel by lowering the temperature at which austenite transformed into martensite [3]. High-manganese steel required a higher austenitizing temperature [4]. High abrasion resistance, including resistance to blows and metal-to-metal wear, had been demonstrated for austenitic high manganese steels. Although it had been observed that components exhibit high wear resistance even without significant mechanical deformation, these steels were designed to harden during use, providing a robust abrasion-resistant surface [5]. These steels were employed in railroad construction as well as mining equipment, including shovels and crushers [6]. This steel was extremely ductile at room temperature, had an austenite microstructure, and stiffened up in response to force [7].

Research conducted globally has examined how alloying and heat treatment might enhance the mechanical characteristics of high manganese steel [8–10]. According to that research, by modifying some alloying elements such as molybdenum (Mo), vanadium (V), and chromium (Cr) in conjunction with the heat treatment methods, this steel may obtain good wear resistance, strength, and hardness properties [11]. Carbides were the most often employed minerals for reinforcement in iron-based alloys, and vanadium carbide (VC) was preferred because of its high hardness, which corresponds to 2600 HV–3000 HV (Vicker hardness) [12]. Vanadium was a powerful carbide-forming element, and it significantly boosted yield strength while reducing ductility in manganese steels. Vanadium was added to manganese steels to precipitation-harden them in concentrations ranging from 0.5% to 2% [13]. Vanadium carbides are stable, and thus higher solution homogenization temperatures of ~1120 °C to ~1175 °C were advised with a typical temperature range of 500 °C to 650 °C [10,14]. Depending on the level of ductility that may be withstood for a specific application, yield strengths of over 700 MPa were achieved [10]. The abrasion resistance of an age-hardened austenitic alloy of nickel, manganese, molybdenum, and vanadium was shown to be inferior to that of the standard grades in tests [5,15]. The VC and V5C6 carbides, which appeared as tiny neutral or hard particles scattered in the austenite grain, were produced when the vanadium level was less than 2% [2,16]. The carbides had a beneficial impact on the wear resistance. On the other hand, the carbides that were scattered along the grain boundaries made the mechanical parts brittle and irreparable.

The ultimate tensile strength, yield strength, hardness at fracture, hardness as quenched, and Charpy V-notch impact are typical mechanical qualities for high manganese steel. This robust steel is unique due to its quick work-hardening, which goes from a yield strength of 379 MPa to an ultimate tensile strength of 965 MPa. Hadfield steel outperforms cast alloy steels, wrought alloy steels, high-chromium steel, tool steels, stainless steels, and white cast irons in gouge abrasion tests. In conclusion, the combination of these characteristics gives high manganese steel greater attributes when operating under gouge abrasion compared to other alloying steels. Hadfield manganese steel may work-harden quickly after being struck. It has been widely employed in a variety of applications because of its special service features, including in dredge buckets, rail tracks, jaw crushers, and a number of high-impact and wear-resistant activities. The steel includes carbides and an embrittling transition product in its as-cast state. Regardless of the cooling rates of the molds, carbides develop in castings that are cooled gradually. When more than 1.0% C is present in the as-cast material or when an alloying element like Cr, V, Ti, etc., is added, these carbides can also develop. If quenching fails to produce quick cooling throughout the full section thickness, they develop in heavy section castings during the heat treatment [17].

The ideal microstructure can be determined by a number of factors, including the alloying components, casting circumstances, solidification rate, microalloying components, and heat treatment cycles. In order to reduce segregation, manage precipitation, and maintain control over the microstructure development during the processing of high-manganese steel, solidification conditions must be carefully taken into account.

Among these above-mentioned factors, casting circumstances are important industrial parameters for generating complex shapes out of a variety of materials. There are two stages

to this process: filling and solidification. Each step is critical in the sound casting process. The filling process is controlled by a metal guidance system that includes a sprue, ingates, pouring cup, and runner. The riser system, on the other hand, is used to feed metal as it shrinks during solidification. When higher efficiency and production quality are required, the casting process is critical [18]. The size of a component in casting can range from small to huge, depending on its size and shape. The casting process begins with the creation of a cavity inside a sand mold, which is subsequently filled with molten metal. The molding and melting processes are the most significant of the casting process's several stages. Casting quality and foundry productivity can both benefit from better control of these operations. The foundry business, in general, relies on skilled personnel and suffers from a dearth of process mechanization. Furthermore, global consumers expect and want defect-free castings delivered on time, which is forever a challenging task for the foundry business [19].

The purpose of the computer modeling of a process is to create forecasts about the effects of changing the process's controls. Shrinkage cavities and other potentially dangerous faults could be predicted using computer software by correctly and quickly simulating the pouring of liquid metal into a mold and its subsequent solidification. It is possible to mimic the changing gating system, volume, position of feeders, and even the casting design. The casting system approach can thus be optimized before the design and casting methods are completed, resulting in time savings during the casting testing phases [20]. Since 1980, numerical simulation software for metal flow and solidification modelling has been available. Several commercial software programs are now available, and they are constantly being updated.

The modeling/simulation of the filling of casting is exponentially more demanding considering that chaotic and quiescent flow is involved in elaborately-shaped casting. The goals of solidification modelling are to predict the location of the shrinkage cavity, determine the solidification array and weights, and calculate the size and volume of all the feeders and gating systems in casting, as well as to compute the sizes and weights of different metals in a solid model, and to produce various levels of quality, allowing designers to ignore or highlight the microporosity level [20].

Some advantages of computer modelling and simulation include improving casting quality, casting yield, and the productivity of castings. The data provides for a certain geometric model regarding weight, surface, and volume, thus permitting a quick cost assessment. Efficiency in engineering design and a general-purpose heat transfer computerized enmeshment simulator enables shorter design durations, fewer trials, and quicker evaluation of engineering advances and implementation [21]. Casting simulation can also help forecast and locate defects. Casting simulation technology was used to thoroughly analyze and optimize the ability of the casting process to feed material. As a result, excellent quality and yield can be obtained without investing in foundry trials. By using simulation techniques for foundry operations, it is possible to reduce product rejection, enhance yield, and boost output, all of which ultimately result in cost savings.

The fluid flow pattern has a direct impact on the solidification behavior and heat transfer of a casting [22]. A quick fluid flow lowers the solidification time, leading to poor mechanical properties. When the gating system's design is altered, the melt flow deviates from the separating line of the mold, changing the pattern of the mold filling [23]. Gate geometry has an impact on the change in the head pressure of the metal at the beginning of the mold cavity. Gate design has an impact on the metal filling, which has a significant effect on the quality of the casting. A homogeneous heat gradient and the restriction of mold erosion are achieved with correct gating, resulting in a smooth metal filling [24]. An improper gating design causes turbulence by forming an oxide film, air entrapment, dross, and sand inclusion [25–31].

Accurate gate shapes and sizes control the pace of molten metal entry, reducing entrapment [32]. Along with solidification, flow pattern, and gating system design, numerous gating configurations can be used to limit mold filling. Among the gating layouts mentioned in the literature are top, bottom, and side gating. Despite the fact that different

strategies and ideas have been offered to improve the gating system [33–44], the issue is still up for dispute. Moreover, it is apparent that each casting requires a unique gating system design and that a wide variety of castings for varied applications cannot be developed using a single gating system design. Because of this, the gating system needs to be specifically designed for each unique form, size, wall thickness, and alloy, among other considerations. However, there have been few analyses on the effect of the gating arrangement on the mechanical characteristics, particularly in the CO_2 sand molding process, and no such investigation has been revealed in the literature. According to the literature, prior studies concentrated on mold filling and its influence on the microstructure of casted components. A deeper investigation of the specific behavior of gating design in CO_2 sand casting is needed. To the best of our knowledge, the impacts of the gating design and riser system on the structure and mechanical characteristics of high manganese steel bushes created using CO_2 sand molding technology, as well as the comparison of conventional manual calculation and SolidCast technique for high manganese steel bushes created using CO_2 sand molding technology, have not been systematically investigated and thus are investigated in this work.

2. Materials and Methods

ZGMn13Cr, a high manganese steel alloy, was employed in this work for CO_2 sand casting owing to its technical relevance. It has long been utilized in mining, metallurgy, building materials, the power sector, and railroads, as well as in cement manufacturing, due to its good work-hardening capacity and toughness under high-load impact and severe stress [45]. The alloy's chemical composition is demonstrated in Table 1. The casting variables were designed using the traditional approach initially. The casting process and mold were then created in accordance with the manual's standards, and the liquid metal was mixed into the mold after the molten metal was constructed following the necessary steel standard.

Table 1. ZG Mn13Cr steel grade's chemical composition.

C%	Si%	Mn%	S%	P%	Cr%	Mo%	Ni%	Al%	Cu%
1.10	0.64	12.00	0.010	0.085	1.60	0.05	0.30	0.042	0.18

The modulus of the casting, represented as, Mc was computed to be ~2.21 cm using the Chvorinov rule. The modulus of the riser, represented as, Mr was measured at ~2.652 cm using a ratio of ~1.2 Mc. Using

$$\mathrm{Mr} = \frac{\mathrm{Vr}}{\mathrm{Ar}} = \frac{\pi \mathrm{R}^2 \mathrm{H}}{2\pi \mathrm{RH} + \pi \mathrm{R}^2} = \frac{\mathrm{RH}}{2\mathrm{H} + \mathrm{R}} = \frac{\mathrm{DH}}{4\mathrm{H} + \mathrm{D}} \quad (1)$$

and a cylindrical riser was estimated with a height to diameter ratio of 1:2.3. The riser had a diameter of 110 mm and a height (H) of 250 mm to meet the riser modulus. Number of Risers = Lc/8Mc + Dr was used to compute the number of risers. The side neck's width (Wn), height (Hn), and length (Ln) were estimated using the calculations below: Ln Maximum of D/3, Hn = 0.6 0.8T, Wn = 2.5Ln + 0.18D Where D is the riser's diameter and T is the casting thickness [46]. The length of the neck was maintained to a minimum to allow for fettling and cleanup. Between the casting and the riser, a neck with dimensions of 60 mm and 40 mm was installed. A down sprue, ingates and runner were the major components of the gating system. The metal penetrated through the runner across the down sprue, which divides the metal to the ingates, and then the metal flowed into the mold via the ingates.

The area ratios of the down sprue to the runner and the runner to the ingates were retained at 1:1.2:1.4 for the gating system, respectively. The sprue had a diameter of 40 mm, the runner had a cross-section of 35 mm × 40 mm, and the ingate had a cross-section of 25 mm × 40 mm. Thermal Modulus analysis was used by SolidCast (8.2.1, Finite Solution,

Hamilton, Ohio 45013, United States). In the present study, the commercially available simulation tool SolidCast 2013 was used. The physical parameters of the simulated process were given in Table 2.

Table 2. The material's physical properties for fluid flow simulations.

Material's Properties	Value
Thermal Conductivity (W/m-K)	25.5
Specific Heat (J/kg-k)	500
Density (kg/m^3)	7690
Initial temperature (°C)	1470
Solidification temperature (°C)	1193
Latent heat of fusion (J/kg)	279,924.9
Freezing Range (°C)	185

The Hazard Modulus of casting Mc was estimated and determined to be 2.56 cm as a consequence of the Riser Design Calculator calculating necked simulation-run casting modules. The ratio for determining the modulus of the riser Mr was preserved at 1.2 Mc and determined to be 3.1 cm. A riser with a height to diameter ratio of 1:11 with a cylindrical form was selected, and a riser with a height of 200 mm and a diameter of 110 mm was computed for 2 nos. of casting. The used neck measured 100 mm in diameter and 45 mm in the distance between the casting and the riser. The down sprue to the runner and the runner to the ingates area ratios for the gating mechanism were kept at 1:1.2:1.75, respectively. The sprue was 30 mm in diameter, the runner was 30 mm in cross section, and the ingate was 15 mm in cross section. In this work, the physical models with an outer diameter of bush: 137 mm, inner diameter: 113 mm, height: 120 mm, mesh size: 6 mm, mesh type: rectangular, and meshing technique: a finite difference method were employed. The fluid took 12 sec to fill the mold. A 2D model of a casting part, a manual method of design of casting, and an optimized gating system after a SolidCast simulation were presented in Figure 1. Silica sand with a SiO_2 content of 95%, Fe_2O_3 content of 1%, and Clay content of 4% were used as a molding sand. Sodium silicate was utilized up to ~7 wt.% as a required ingredient. The mold was filled with CO_2 gas, which created silica gel and hardened it. In the CO_2 molding process, molding sand is mixed with sodium silicate. The mixture is loosely rammed into the mold around the pattern. CO_2 gas is forced into the mold. CO_2 reacts with the sodium silicate and produces silica gel by the following reaction:

$$Na_2SiO_3 + CO_2 \rightarrow Na_2CO_3 + SiO_3.xH_2O \text{ (Silica gel)} \quad (2)$$

Steel was produced using a 3 ton electric arc furnace. Table 3 displays the gating system's casting weight, melting and pouring temperatures, and mold-filling velocities.

Table 3. Parameter calculations for casting.

Parameter	Value
Casting's Net weight (kg)	7
Pouring Temperature (°C)	1410
Melting Temperature (°C)	1375
Pouring time (s)	16
Pouring rate (kg/s)	4.6
Mold filling velocity of gate (mm/s)	891.7

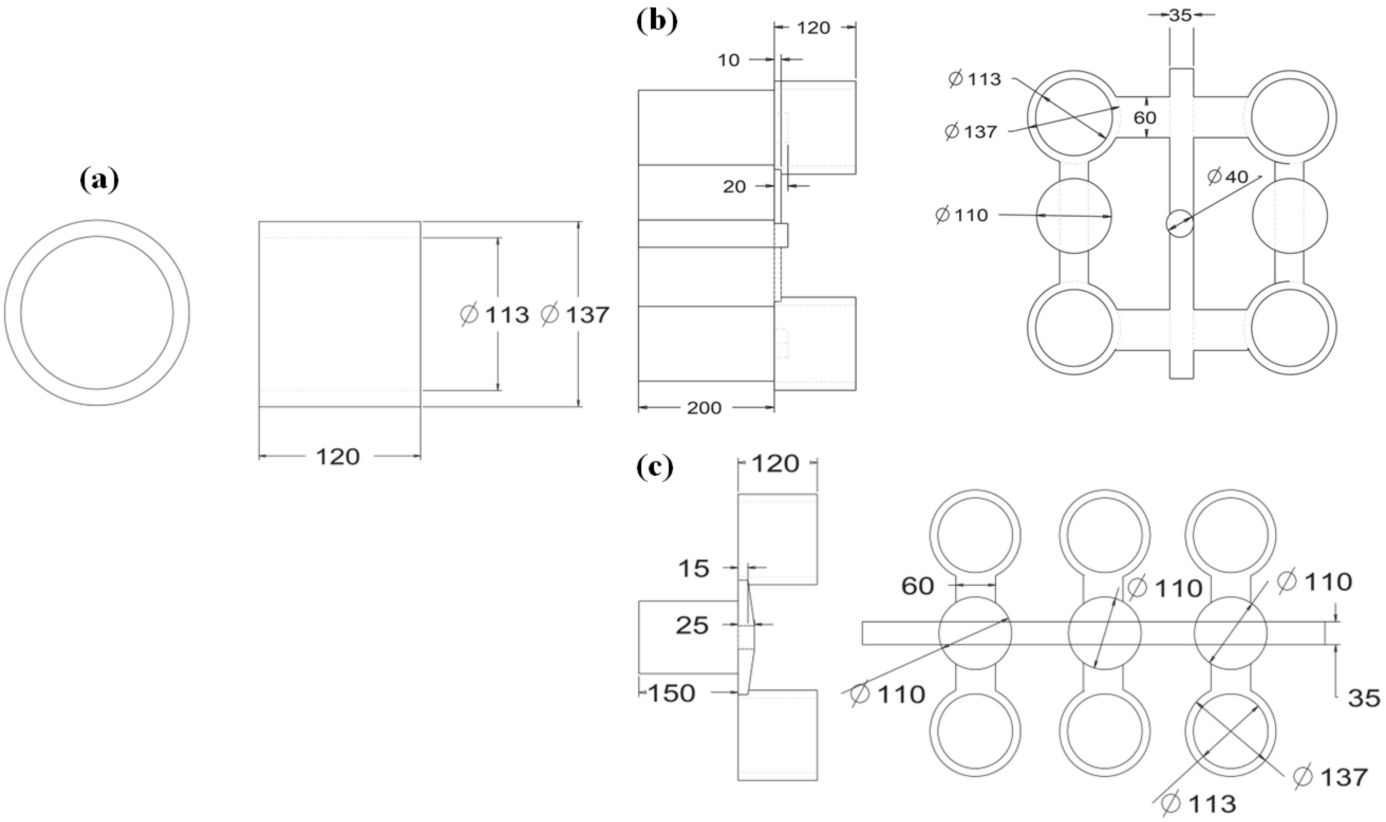

Figure 1. (**a**) A 2D model of a casting part; (**b**) a gating system design using a manual method calculation (all dimensions are in mm); and (**c**) a gating system design using the SolidCast simulation method (all dimensions are in mm).

A pneumatic chisel was used to remove the casting from the mold once it had fully solidified to a certain temperature. The riser and gating were taken out of the casting using a grinder's cutting disc. The casting surfaces were ground smooth using a grinder. The casting variables were generated with the SolidCast simulation program, and the complete fabrication process [47] was replicated, as presented in Figure 2.

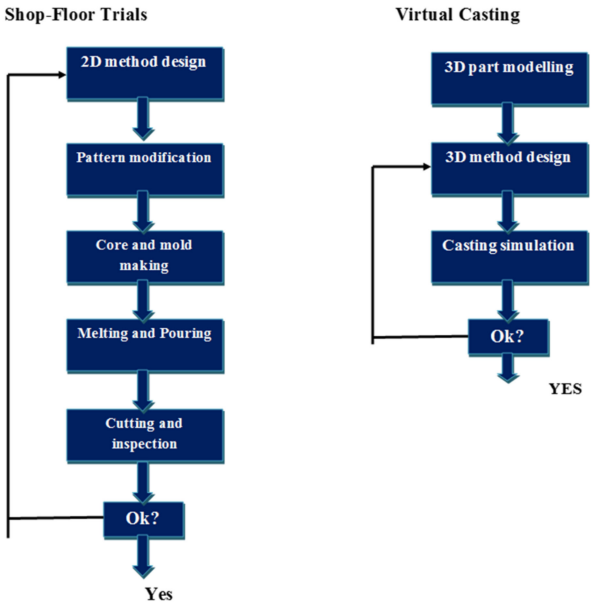

Figure 2. The production steps of a typical sand-casting process.

3. Result and Discussions

The manual procedure was used to develop the casting technology. The Chvorinov rule and the volume over surface area technique were used to estimate the risers, while the gating system was manually calculated. For the production of bush, a wooden pattern is made as per the designed gating system shown in Figure 3a,b. When the risers were removed from the castings, the region close to the risers, as illustrated in Figure 3c, shrunk significantly. This occurred as a result of the risers not being supplied to the casting in a large enough quantity. The section thickness difference at the meeting of separate casting surface regions caused shrinkage where hot spots were expected to develop [48]. Because the freezing range of solidification causes macroporosity to gradually convert into microporosity, there is no essential difference between these two forms of porosities. The appearance of macroporosity can range from multiple shrinkage holes to a single cavity with a rough surface. Macroporosity occurs largely in isolated hot areas that are often positioned at junctions, the midst of thick sections, and corners.

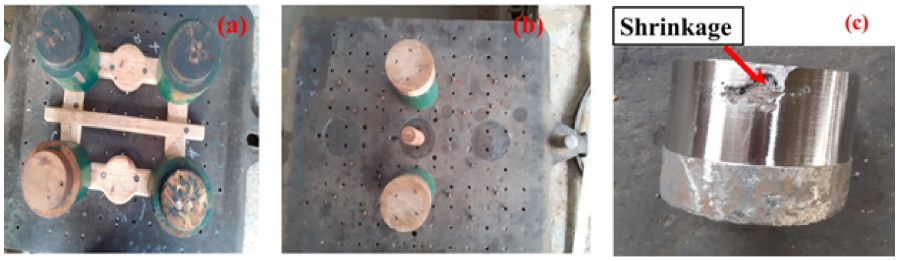

Figure 3. (**a**) and (**b**) Pattern after traditional method (**c**) Shrinkage was seen in a casting created using the manual technique.

The casting model was updated using SolidCast [49] to remove these faults for sound casting production and to increase casting quality. Different aspects, such as the riser and gating system design, were investigated for this purpose. The riser design tool was used to create an optimum riser with the highest serving capacity. The gating system was designed using the Gating Design tool to ensure the appropriate metal flow velocity within the mold. As shown schematically in Figure 3, two castings were placed in a single mold to spread the equal flow and pressure of the metal in the mold. The modified model was simulated again, and the metal flow was validated by applying the SolidCast FlowCast module. After simulation, the metal's density factor for shrinkage was evaluated utilizing the FCC criterion, and the microporosity was tested. The improved simulated model works well, as shown in Figure 4a,b.

It can be seen from the simulated pattern that there is no microporosity and shrinkage. The wooden pattern is designed as shown in Figure 5a, and the casting was empirically cast according to the intended parameters using SolidCast software and shown in Figure 5b–d for additional validation of these simulated outcomes given in Figure 4a,b. The photographs demonstrated that there was no shrinkage near risers, as well as no evidence of microporosity (see Figure 5d). As a result, the SolidCast results were proven to be accurate.

Optical microscopy was used to examine experimentally cast samples' microstructure with optimum parameters, as shown in Figure 6a,b. The outcomes display the black precipitate area and the white matrix region. The white matrix represents the austenitic structure, whereas the black precipitate represents the pearlite structure. SEM was used to investigate the microstructure of the experimentally-casted specimen with improved settings, and the findings are shown in Figure 6c. Figure 6c shows that the micrographs have no visible voids or microporosity. This indicates that the casted samples are sound and free of flaws. Based on these findings, it's possible that these models will have improved mechanical properties.

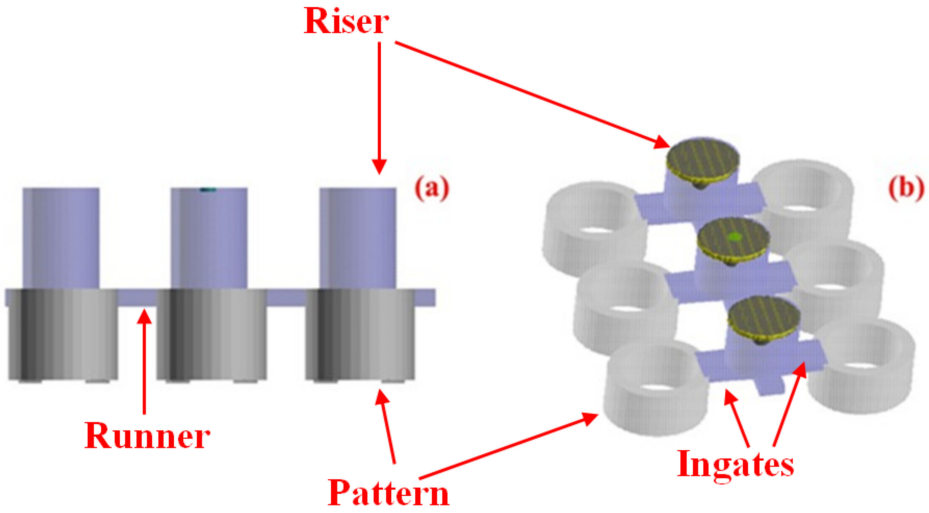

Figure 4. (**a**) The revised gating system design by SolidCast. (**b**) No shrinkage or microporosity was found in the simulation.



Figure 5. (**a**) The wooden pattern; (**b**) casting with the risers and gating system designed by SolidCast; (**c**) after fettling; and (**d**) after machining.

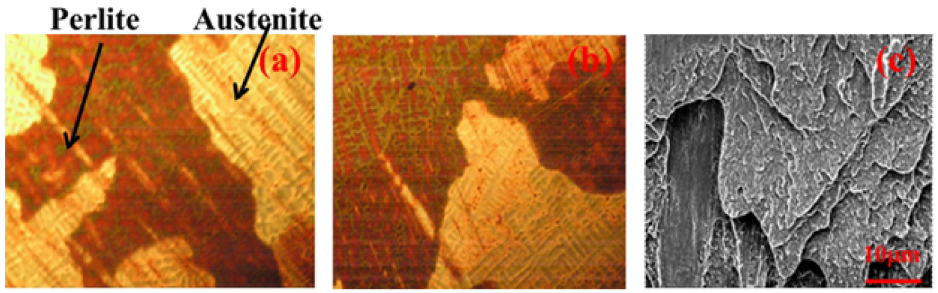

Figure 6. (**a**) and (**b**) Optical microscopy images (**c**) SEM micrograph of casted sample.

In Figure 7, a comparison of the mechanical testing of the manual and SolidCast simulated specimens was carried out. The yield strength of the specimen prepared by the modified SolidCast rose dramatically from 425 MPa for the manual approach to 563 MPa for the revamped SolidCast. Similarly, the specimen's tensile strength and hardness were higher after using the revised riser and gating system. The void and defect-free microstructure of the specimen that was attained by applying a revised riser and gating system might be linked to the improvement in mechanical characteristics. The shrinkage and

microporosity reported by the visual and SolidCast simulations might be attributed to the manually-computed riser and gating system's low mechanical characteristics (see Figure 3). Microstructural studies and mechanical properties corroborate the findings.

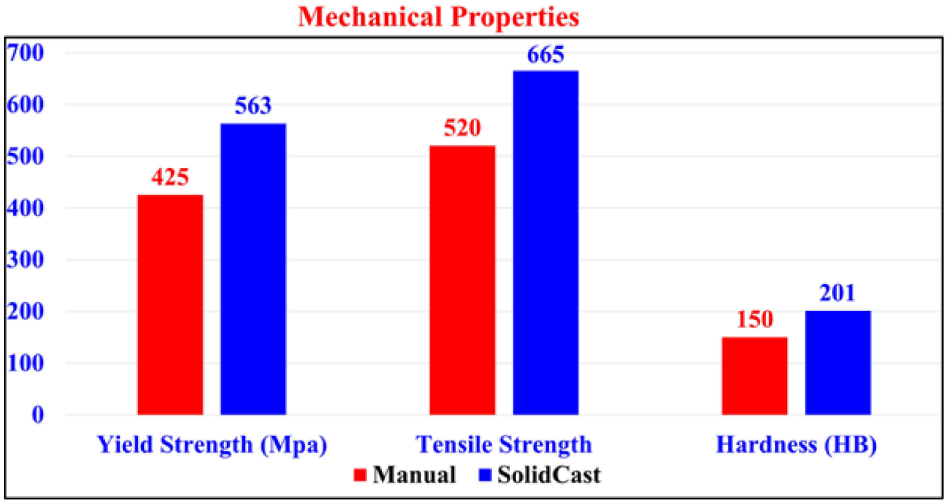

Figure 7. Graphic representation for the comparison of Hardness, Yield, and Tensile Strength.

Figure 8 displayed the riser, gating weight, gross weight, and liquid weight of the sample cast by the manual approach and the simulation approach using SolidCast software. The total weight and liquid metal weight were strongly affected by the riser and gating system design. By employing the SolidCast simulation method, the sample casted through a revised riser and gating system used less liquid metal, lowering the overall manufacturing cost. The weight distribution chart (with respect to one Bush) shows that the weight of risers and runners was reduced from 9.25 kg to 7.12 kg and the overall liquid weight was reduced from 16.25 kg to 14.12 kg using SolidCast simulation software. In consequence, casting yield was improved from ~43% to ~50%.

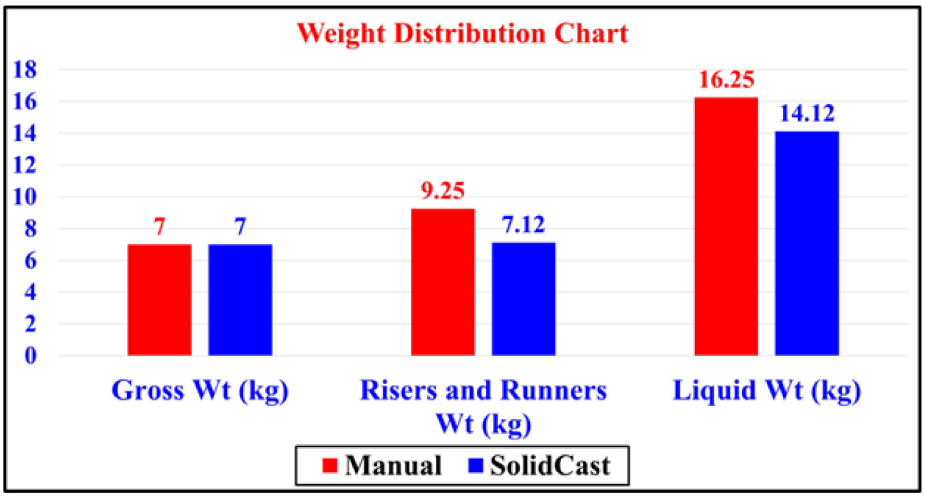

Figure 8. Graphic representation for the comparison of Riser and Gating weight, Gross weight, and liquid weight by Manual and SolidCast Simulation.

In industry, the cost analysis of the procedure is also critical. The entire cost (material, labor, and overheads) for the bush casted is greatly decreased by an improved riser and gating system utilizing the SolidCast simulation method. In terms of the fixed and variable expenses, the fabrication costs were significantly cut by an amount of ~8%.

4. Conclusions

This study looked into the gating design and riser system effects on mechanical characteristics of high manganese steel bush samples manufactured by a CO_2 sand molding technique. Moreover, both the traditional manual methods and the SolidCast simulation methods were used to design the gating and riser systems. A systematic experiment was used to authenticate the calculated and simulation results. A visual check found major shrinkage in manually-designed castings, whereas software-structured castings looked to be in relatively good form, with no micro porosity and no shrinkage (macroporosity). The validity of software-designed castings with optimum parameters is further proven by optical microscopy and SEM examination. Microstructural research appears to be in agreement with the behaviour of mechanical property. Software-structured castings with optimum parameters had a yield strength of around 563 MPa, equated to manual-designed castings, which had a yield strength of 425 MPa. Considerable gains of around 27% in tensile strength and 34% in hardness were also reported for defect-free software-structured castings with optimal parameters. Furthermore, sound casting considerably decreased the rate of disapproval, cutting total production costs. Casting simulation helped to predict and locate the defects. With the casting simulation technique, the feed ability of the casting process was systematically studied and optimized. Hence, high quality and yield were obtained without the expense of foundry trials. By applying simulation techniques in foundry procedures, the prevention of product rejection and an increase in yield and production can be achieved, which ultimately results in cost reduction.

Author Contributions: Conceptualization, H.A., R.A.M. and F.A.; Methodology, F.A.; investigation, F.A. and R.A.M.; formal analysis, F.A. and R.A.M.; Writing—Original draft preparation, F.A. and R.A.M.; supervision, R.A.M. and H.A.; Writing- Reviewing and Editing, H.A. and I.A. All authors have read and agreed to the published version of the manuscript.

Funding: This research received no external funding.

Data Availability Statement: All data is included in the manuscript.

Acknowledgments: The authors extend their appreciation to the Deputyship for Research & Innovation, Ministry of Education in Saudi Arabia for funding this research work through the project number (IFPSAU-2021/01/18816).

Conflicts of Interest: The authors declare no conflict of interest.

References

1. Srivastava, A.K.; Das, K. Microstructural characterization of Hadfield austenitic manganese steel. *J. Mater. Sci.* **2008**, *43*, 5654–5658. [CrossRef]
2. Moghaddam, E.G.; Varahram, N.; Davami, P. On the comparison of microstructural characteristics and mechanical properties of high-vanadium austenitic manganese steels with the Hadfield steel. *Mater. Sci. Eng. A* **2012**, *532*, 260–266. [CrossRef]
3. Feng, X.Y.; Zhang, F.C.; Yang, Z.N.; Zhang, M. Wear behaviour of nanocrystallised Hadfield steel. *Wear* **2013**, *305*, 299–304. [CrossRef]
4. Karaman, I.; Sehitoglu, H.; Chumlyakov, Y.I.; Maier, H.J.; Kireeva, I.V. The effect of twinning and slip on the Bauschinger effect of Hadfield steel single crystals. *Metall. Mater. Trans. A* **2001**, *32*, 695–706. [CrossRef]
5. Kusakin, P.; Tsuzaki, K.; Molodov, D.A.; Kaibyshev, R.; Belyakov, A. Advanced thermomechanical processing for a high-Mn austenitic steel. *Metall. Mater. Trans. A* **2016**, *47*, 5704–5708. [CrossRef]
6. LI, X.; Wang, C.; Lu, L.U. Microstructure and impact wear resistance of TiN reinforced high manganese steel matrix. *J. Iron Steel Res. Int.* **2012**, *19*, 60–65.
7. Dingshan, L.; Zhongyi, L.; Wei, L. Influence of carbon content on microstructure and mechanical properties of Mn13Cr2 and Mn18Cr2 cast steels. *China Foundry* **2014**, *11*, 173–178.
8. Wen, Y.H.; Peng, H.B.; Si, H.T.; Xiong, R.L.; Raabe, D. A novel high manganese austenitic steel with higher work hardening capacity and much lower impact deformation than Hadfield manganese steel. *Mater. Des.* **2014**, *55*, 798–804. [CrossRef]
9. Mishra, S.; Chaubey, A.; Mandal, A. Effect of Heat Treatment on the Microstructure of Mg-4Al-Nd Alloys. *Technologies* **2017**, *5*, 23. [CrossRef]
10. Pham, M.K.; Nguyen, D.N.; Hoang, A.T. Influence of Vanadium Content on the Microstructure and Mechanical Properties of High-Manganese Steel. *Int. J. Mech. Mechatron. Eng.* **2018**, *18*, 141–147.

11. Hazeli, K.; Askari, H.; Cuadra, J.; Streller, F.; Carpick, R.W.; Zbib, H.M.; Kontsos, A. Microstructure-sensitive investigation of magnesium alloy fatigue. *Int. J. Plast.* **2015**, *68*, 55–76. [CrossRef]
12. Holtzer, M.; Bobrowski, A.; Drożyński, D.; Mocek, J. Investigations of protective coatings for castings of high-manganese cast steels. *Arch. Foundry Eng.* **2013**, *13*, 39–44. [CrossRef]
13. Beladi, H.; Nuhfer, N.T.; Rohrer, G.S. The five-parameter grain boundary character and energy distributions of a fully austenitic high-manganese steel using three-dimensional data. *Acta Mater.* **2014**, *70*, 281–289. [CrossRef]
14. Kim, J.-K.; Chen, L.; Kim, H.-S.; Kim, S.-K.; Estrin, Y.; Cooman, B.C.D. On the tensile behavior of high-manganese twinning-induced plasticity steel. *Metall. Mater. Trans. A* **2009**, *40*, 3147. [CrossRef]
15. Lindroos, M.; Apostol, M.; Heino, V.; Valtonen, K.; Laukkanen, A.; Holmberg, K.; Kuokkala, V.T. The deformation, strain hardening, and wear behavior of chromium-alloyed hadfield steel in abrasive and impact conditions. *Tribol. Lett.* **2015**, *57*, 24. [CrossRef]
16. Wei, S.; Jinhua, Z.; Liujie, X.; Rui, L. Effects of carbon on microstructures and properties of high vanadium high-speed steel. *Mater. Des.* **2006**, *27*, 58–63. [CrossRef]
17. Ham, Y.S.; Kim, J.T.; Kwak, S.Y.; Choi, J.K.; Yoon, W.Y. Critical cooling rate on carbide precipitation during quenching of austenitic manganese steel. *China Foundry* **2010**, *7*, 177–182.
18. Liu, F. Optimized Design of Gating/Riser System in Casting Based on CAD and Simulation Technology. Master's Thesis, Worcester Polytechnic Institute, Worcester, MA, USA, 2009.
19. Mane, V.V.; Sata, A.; Khire, M.Y. New approach to casting defects classification and analysis supported by simulation. In Proceedings of the 59th Indian Foundry Congress & International Foundry Exhibition (IFEX 2011), Chandigarh, India, 12 February 2011.
20. Brown, J.R. *Foseco Ferrous Foundryman's Handbook*, 11th ed.; Elsevier Ltd.: Amsterdam, The Netherlands, 2000.
21. Viswanathan, S.; Apelian, D.; Donahue, R.J.; DasGupta, B.; Gywn, M.; Jorstad, J.L.; Monroe, R.W.; Sahoo, M.; Prucha, T.E.; Twarog, D. *ASM Handbook Volume 15: Casting*; ASM International: Almere, The Netherlands, 2008.
22. Mirbagheri, S.; Shrinparvar, M.; Ashory, H.; Davami, P. Simulation of surface roughness on the flow pattern in the casting process. *Mater. Des.* **2004**, *25*, 655–661. [CrossRef]
23. Masoumi, M.; Hu, H.; Hedjazi, J.; Boutorabi, M. Effect of gating design on mold filling. *Trans. Am. Foundry Soc.* **2005**, *113*, 185–196.
24. Rajput, R.K. *A Textbook of Manufacturing Technology: Manufacturing Processes*; Laxmi Publication Pvt Ltd.: Delhi, India, 2007.
25. Hu, B.; Tong, K.; Niu, X.P.; Pinwill, I. Design and optimisation of runner and gating systems for the die casting of thinwalled magnesium telecommunication parts through numerical simulation. *J. Mater. Process. Technol.* **2000**, *105*, 128–133. [CrossRef]
26. Devendar, G.; Kumar, K.S.; Reddy, A.C. Modification of gating system for proper mould filling of bracket casting using procast. In Proceedings of the International Conference on Advanced Materials and manufacturing Technologies (AMMT), Shenzhen, China, 23–24 August 2014; pp. 249–253.
27. Smith, R.W.; DeMonte, A.; Mackay, W.B.F. Development of high-manganese steels for heavy duty cast-to-shape applications. *J. Mater. Process. Technol.* **2004**, *153*, 589–595. [CrossRef]
28. Yang, D.; Li, S.; He, F.; Sung, W.; Kao, J.; Chen, R. Twin gating system design for typical thin wall stainless steel castings based on fast pouring mechanism. *Front. Mech. Eng. Mater. Eng. II* **2014**, *457–458*, 1657–1660. [CrossRef]
29. Pawliczek, A.; Vladik, V. Impact of electric power prices on total costs of foundry casting production with the side effect on global competitiveness. In Proceedings of the 23rd International Conference on Metallurgy and Materials Metal, Brno, Czech Republic, 21–23 May 2014; pp. 1558–1563.
30. Ducic, N.; Slavkovic, R.; Milicevic, I.; Cojbasic, Z.; Manasijevic, S.; Radisa, R. Optimization of the gating system for sand casting using genetic algorithm. *Int. J. Metalcast.* **2017**, *11*, 255–265. [CrossRef]
31. Fourie, J.; Lelito, J.; Zak, P.; Krajewski, P.; Wolczynski, W. Numerical optimization of the gating system for an inlet valve casting made of titanium alloy. *Arch. Metall. Mater.* **2015**, *60*, 2437–2446. [CrossRef]
32. Wang, T.; Yao, S.; Tong, Q.; Sui, L. Improved filling condition to reduce casting inclusions using the submerged gate method. *J. Manuf. Process.* **2017**, *27*, 108–113. [CrossRef]
33. Hawranek, R.; Lelito, J.; Suchy, J.; Zak, P. The simulation of a liquid cast iron flow through the gating system with filter. *Arch. Metall. Mater.* **2009**, *54*, 351–358.
34. Huang, P.; Lin, C. Computer-aided modeling and experimental verification of optimal gating system design for investment casting of precision rotor. *Int. J. Adv. Manuf. Technol.* **2015**, *79*, 997–1006. [CrossRef]
35. Modaresi, A.; Safikhani, A.; Noohi, A.; Hamidnezhad, N.; Maki, S. Gating system design and simulation of gray iron casting to eliminate oxide layers caused by turbulence. *Int. J. Metalcast.* **2017**, *11*, 328–339. [CrossRef]
36. Campbell, J. Stop pouring, start casting. *Int. J. Metalcast.* **2012**, *6*, 7–18. [CrossRef]
37. Campbell, J. Cavitation in liquid and solid metals: Role of bifilms. *Mater. Sci. Technol.* **2015**, *31*, 565–572. [CrossRef]
38. Campbell, J. Sixty years of casting research. *Metall. Mater. Trans. A* **2015**, *46A*, 4848–4853. [CrossRef]
39. Jezierski, J.; Dojka, R.; Janerka, K. Optimizing the gating system for steel castings. *Metals* **2018**, *8*, 266. [CrossRef]
40. Yin, J.; Ersson, M.; Mao, H.; Jönsson, P.G. Mathematical modelling of the initial mold filling with utilization of an angled runner. *Metals* **2019**, *9*, 693. [CrossRef]
41. Sama, S.R.; MacDonald, E.; Voigt, R.; Manogharan, G. Measurement of metal velocity in sand casting during mold filling. *Metals* **2019**, *9*, 1079. [CrossRef]

42. Papanikolaou, M.; Pagone, E.; Jolly, M.; Salonitis, K. Numerical simulation and evaluation of campbell running and gating systems. *Metals* **2020**, *10*, 68. [CrossRef]
43. Majernik, J.; Gaspar, S.; Kmec, J.; Karkova, M.; Mascenik, J. Possibility of utilization of gate geometry to modify the mechanical and structural properties of castings on the Al-Si basis. *Materials* **2020**, *13*, 3539. [CrossRef]
44. Gašpár, Š.; Corani, T.; Majerník, J.; Husár, J.; Číková, L.K.; Gojdan, D.; Paško, J. Influence of gating system parameters of die-cast molds on properties of Al-Si castings. *Materials* **2021**, *14*, 3755. [CrossRef]
45. Zhou, Z.; Zhang, Z.; Shan, Q.; Li, Z.; Jiang, Y.; Ge, R. Influence of heat-treatment on enhancement of yield strength and hardness by Ti-V-Nb alloying in high-manganese austenitic steel. *Metals* **2019**, *9*, 299. [CrossRef]
46. Heine, R.W.; Loper, C.R.; Rosenthal, P.C. *Principles of Metal Casting*; McGraw-Hill: New York City, NY, USA, 1955.
47. Alrobei, H.; Malik, R.A.; Hussain, A.; Alzaid, M.; Farhat, L.B.; Badruddin, I.A. Effects of gating design on structural and mechanical properties of high manganese steel by optimizing casting process parameters. *J. Mech. Sci. Technol.* **2022**, *36*, 3931–3937. [CrossRef]
48. Li, J.; Chen, R.; Ma, Y.; Ke, W. Characterization and prediction of microporosity defect in sand cast WE54 alloy castings. *J. Mech. Sci. Technol.* **2014**, *30*, 991–997. [CrossRef]
49. Muenprasertdee, P. Solidification Modelling of Iron Castings Using SOLIDCast. Master's Thesis, West Virginia University, Morgantown, WV, USA, 2007.

Disclaimer/Publisher's Note: The statements, opinions and data contained in all publications are solely those of the individual author(s) and contributor(s) and not of MDPI and/or the editor(s). MDPI and/or the editor(s) disclaim responsibility for any injury to people or property resulting from any ideas, methods, instructions or products referred to in the content.